Sintering behavior of two roughened crystals just after contact

Robert S. Farr*
Unilever R&D, Olivier van Noortlaan 120, AT3133, Vlaardingen, The Netherlands

Martin J. Izzard
Unilever R&D, Colworth House, Sharnbrook, Bedford MK44 1LQ, England

(Received 6 December 2007; published 24 April 2008)

We consider two spherical, roughened crystals with approximately isotropic surface free energy, which are brought into contact and begin to sinter. We argue that the geometry immediately postcontact is two dimensional and Cartesian and can be approximated by the evolution of a slot-shaped cavity. On this basis, we construct traveling wave solutions for the crystal shape in the limits of bulk- and surface-diffusion-limited kinetics. These solutions are then used to calculate scalings for the neck size as a function of time t after contact: We predict that neck size is proportional to $t^{1/4}$ for the bulk-diffusion-limited case and (following a single pinch-off event) approximately proportional to $t^{1/3}$ for the surface-diffusion-limited case.

DOI: 10.1103/PhysRevE.77.041608 PACS number(s): 81.10.Aj

I. INTRODUCTION

A crystal in equilibrium against its vapor or a melt eventually reaches a shape that can be obtained by the Wulff construction [1]: Let the free energy per unit area of a plane surface of the crystal which is perpendicular to a unit vector $\hat{\mathbf{n}}$ be given by $\gamma(\hat{\mathbf{n}})$. We define the points $\mathbf{p}(\hat{\mathbf{n}}) \propto \hat{\mathbf{n}}\gamma(\hat{\mathbf{n}})$ for some fixed constant of proportionality which eventually sets the size of the crystal. Next we construct a plane through each $\mathbf{p}(\hat{\mathbf{n}})$, perpendicular to $\hat{\mathbf{n}}$. The Wulff shape of the crystal is the inner envelope of all such planes.

From the terrace-ledge-kink [2,3] model we expect the surface free energy of a crystal to have cusplike minima near to the crystallographic symmetry directions: For a plane oriented at a small angle θ_v to a crystallographic axis (i.e., a "vicinal plane") and at absolute temperature T, the surface free energy per unit area behaves as [4]

$$\gamma(\theta_v, T) \approx \gamma_0(T) + \frac{\sigma(T)}{d_m^2}|\tan\,\theta_v|, \tag{1}$$

where γ_0 is the free energy per unit area of a molecularly flat surface with $\theta_v = 0$, while σ is the ledge energy per molecule and d_m is a molecular distance.

Using the Wulff construction, this leads to the emergence of crystal facets at equilibrium, in which a macroscopic portion of the crystal surface is molecularly flat, save for isolated single-molecule islands and surface vacancies [5]. However, at a particular temperature (the "equilibrium roughening" or "surface melting" temperature), the free energy barrier to formation of new molecular islands on the facet vanishes; the facets become rough on a molecular scale, so that the relevant cusp in the surface free energy disappears along with the facet, to be replaced by a macroscopically smooth, rounded crystal surface [5,6]. This roughening transition is different for different crystallographic symmetry directions; for example three different temperatures have been observed for helium crystals [7], while for ice the basal facet persists up until melting, while prism planes roughen at −2 °C when against vapor [8] or −16 °C when against water under pressure [9]. If the crystal surface is not at equilibrium, but instead growing, this can move the roughening transition to lower temperatures [10,11].

In this investigation, we start from two assumptions: First, we assume that all the relevant crystallographic planes are roughened (there may, however, be other directions not involved in the analysis described below, which are faceted). Second, we make the approximation that the roughened portion of a crystal surface has a fairly isotropic surface free energy per unit area γ (a typical approximation for phase-field studies of dendritic growth [12] or solvability theory [13]).

When a roughened crystal does not have its Wulff shape, then the surface free energy will not be equal everywhere. The chemical potential μ of a molecule at a curved surface differs from the value μ_0 it would have for a flat surface by the well-known Gibbs-Thomson relation, which in linearized form gives

$$\mu = \mu_0 + \Omega_v \kappa \gamma. \tag{2}$$

Here Ω_v is the molecular volume and κ is the mean curvature of the surface (positive if the surface is convex).

Molecules will therefore have a tendency to leave convex portions of the surface and attach to concave (or less convex) regions. In doing so, they may either travel through the bulk of the material outside the crystal, in a process of evaporation-condensation (or solution-precipitation for a crystal against a melt), or they may diffuse along the crystal surface [14]. This leads to the crystal surface having a normal velocity v_n, which will in general be the sum of a component v_n^B from molecules arriving by diffusion through the bulk and v_n^S from those arriving along the surface. In Secs. II and III we consider limiting cases where only one of these mechanisms predominates. For vapor phase sintering, it is likely that surface diffusion will dominate, while for liquid phase sintering bulk diffusion may be the important mode [14]. The case where crystal facets interfere [15] has been

*robert.farr@unilever.com

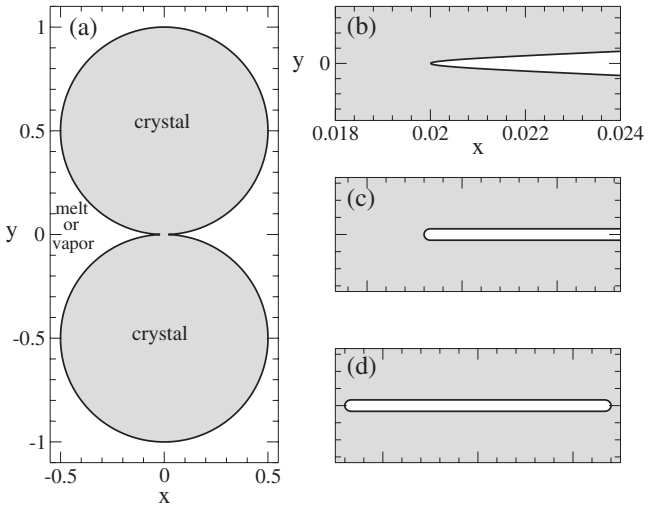

FIG. 1. (a) Schematic of two spherical crystals that are in contact and have started to sinter together, forming a narrow neck of radius $r_n=0.02$ (where all distances are scaled by a suitable capillary length). The crystals are axisymmetric about an axis up the page. (b) Magnified portion of the neck region, illustrating that at the very earliest stages of sintering, the surfaces of the two crystals are nearly parallel close to the neck. (c) Two-dimensional (2D) slot-shaped cavity, with exactly parallel surfaces, which we use as an approximation to the axisymmetric geometry in (b). (d) 2D slot-shaped cavity of finite length, which is more appropriate for simulations.

the subject of more recent work, but is not our concern in this paper.

Consider now two crystals which are close to their equilibrium shapes (and therefore close to being spherical at least in the region of interest). If these crystals are brought into gentle contact, the curvature near the contact point will be large and negative, and therefore a neck will appear and rapidly grow. There will usually be a grain boundary coincident with this neck, but in contrast to Ref. [14], where equilibrium is approached from an initial dihedral angle of π rad, in the case of two sintering crystals, the initial dihedral angle is 0, and we no longer expect grain boundary grooving [14].

The initial stages of neck growth occur rapidly, but nevertheless can be of importance in the rheology of crystal slurries, where contacts may be formed and broken in rapid succession. Relevant examples might include the flow of lava [16] or of brash ice [17]. The initial growth of necks between two crystals has been analyzed previously, for example in Ref. [18], where a $\tilde{t}^{1/3}$ time dependence for neck radius as a function of time $\tilde{t}$ after contact was found for the case of bulk-diffusion-limited growth.

For the development of this paper, we note that there is a geometrical simplification which occurs in the earliest stages of neck growth and which appears to have been overlooked in the literature: If we consider two crystals just after they have touched (Fig. 1), the parts of the surface near the contact point (except for the very high-curvature neck) are very nearly parallel to one another. This suggests that an interesting geometry for investigating the early stages of neck growth is a two-dimensional slot-shaped cavity, illustrated in Fig. 1(c). The closer in time we are to first contact, the better this is as an approximation. Furthermore, if the radius of the neck is large compared to the separation of these two nearly parallel surfaces (as is indeed the case at early times), then the difference between axisymmetric cylindrical coordinates and plane Cartesian coordinates becomes negligible.

In Secs. II and III we analyze a slot-shaped cavity of this kind, and then compensate for the remaining differences between cylindrical and plane Cartesian geometry during structure evolution by invoking conservation of volume. In this way, we obtain the geometry of the crystals in the earliest moments after contact, and also predictions for the scaling behavior of the neck size as a function of time after contact.

II. BULK-DIFFUSION-LIMITED CASE

Consider the case where growth is limited by bulk diffusion to and from the crystal surfaces (attachment kinetics being unimportant because the crystals are roughened). We assume that the mean free path for bulk diffusion is small compared to the feature sizes of interest. If $\phi(\mathbf{r})$ is the volume fraction in the vapor or melt of the type of molecules that can make up the crystal, then this quantity obeys a diffusion equation with a diffusivity D. We make the further approximation that the transients of this equation have died out, so that the concentration field ϕ obeys Laplace's equation

$$\nabla^2\phi = 0. \tag{3}$$

This requires that the surface normal velocity v_n should be small compared to D divided by a typical feature size.

The normal velocity v_n of the crystal surface (which we denote by the set of points S) is obtained by conservation of volume for the crystallizing material:

$$v_n = v_n^B = D\left.\frac{\partial\phi(\mathbf{r})}{\partial\hat{\mathbf{n}}}\right|_{\mathbf{r}\in S}, \tag{4}$$

where $\hat{\mathbf{n}}$ is an outward unit normal vector to S.

We note in passing that we can apply the divergence theorem directly to Eqs. (4) and (3) with the result that the volume of an enclosed cavity is conserved under this evolution, while for a discrete crystal in an open volume of vapor or melt, one must also consider the concentration at infinity before it is possible to say anything about conservation of crystal volume.

Let $\phi_0(T)$ be the concentration of molecules in the melt or vapor that is present at equilibrium against a flat crystal surface at temperature T; then by perturbing this linearly using Eq. (2), we find that the actual concentration at the surface of a curved crystal is given by

$$\phi(\mathbf{r}\in S,T) = \phi_0(T) + \frac{\Omega_v T\gamma\kappa}{L}\frac{d\phi_0}{dT}, \tag{5}$$

where L is the latent heat per unit volume of fusion or evaporation. Equations (3)–(5) determine the evolution of the system in an exactly analogous manner to the Lifshitz-Slyozov-Wagner theory of Ostwald ripening [19–21].

Suppose the coordinates of a point in space are denoted by $(\tilde{x},\tilde{y},\tilde{z})$ and time after contact by $\tilde{t}$. We define a capillary

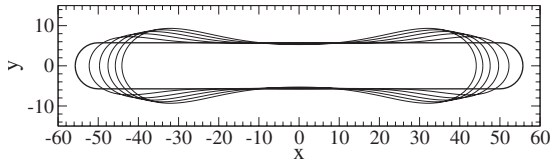

FIG. 2. Numerical solution for the bulk-diffusion-limited evolution of a parallel-sided two-dimensional slot-shaped cavity in a crystal. The initial surface is shown in bold, and subsequent points in time show the formation of dumbbell ends to the curve. Although not shown, the final equilibrium shape must be a circle at the origin containing the same area as the initial curve.

length $l_c \equiv \gamma\Omega_v/L$ and dimensionless space, time, and concentration variables $x=\tilde{x}/l_c$, $t=\tilde{t}TD(d\phi_0/dT)/l_c^2$, and $\psi=(\phi-\phi_0)/(T\,d\phi_0/dT)$. Equations (3)–(5) then take the following simple form in two-dimensional Cartesian coordinates:

$$\left(\frac{\partial^2}{\partial x^2}+\frac{\partial^2}{\partial y^2}\right)\psi(x,y,t)=0, \tag{6}$$

$$\psi[x,y_0(x,t),t]=\frac{\partial^2 y_0/\partial x^2}{[1+(\partial y_0/\partial x)^2]^{3/2}}, \tag{7}$$

$$\frac{\partial y_0}{\partial t}=-\left.\frac{\partial y_0}{\partial x}\frac{\partial \psi}{\partial x}\right|_{y=y_0}+\left.\frac{\partial \psi}{\partial y}\right|_{y=y_0}, \tag{8}$$

where $y=y_0(x)$ is the crystal surface S.

If we solve Eqs. (6)–(8) numerically, using a simple explicit time-stepping scheme for an initial slot-shaped cavity, we see from Fig. 2 that dumbbell-shaped ends start to appear as the cavity evolves toward its eventual equilibrium shape, which must be a circle. This behavior suggests that there may be a traveling wave solution to Eqs. (6)–(8) which propagates at constant velocity v and without change of shape. This solution would consist of a teardrop-shaped cavity formed from the evolution of a semi-infinite slot-shaped cavity in which the parallel surfaces almost, but do not quite, touch. To picture this slot, imagine the initial cavity of Fig. 2, but with two changes: First, let it extend from $x=-\infty$ to 0, rather than the range $x=-56$ to 56 (as shown in Fig. 2). Second, let it be very narrow, rather than extending between $y=-6$ and 6 (as shown in Fig. 2).

If such a solution exists, then it is natural to tackle Eqs. (6)–(8) through complex analysis. Let

$$z \equiv x+iy; \tag{9}$$

then if ψ is an analytic function of z (with an additional time dependence), Eq. (6) is satisfied as an identity, which simplifies the problem greatly.

By balancing leading powers, we find that $\psi(z,t)$ must have a branch point and the solution must be (up to translational symmetry) of the form

$$\psi(z,t) \equiv v^{1/2}\hat{\psi}[v^{1/2}(z+vt);a], \tag{10}$$

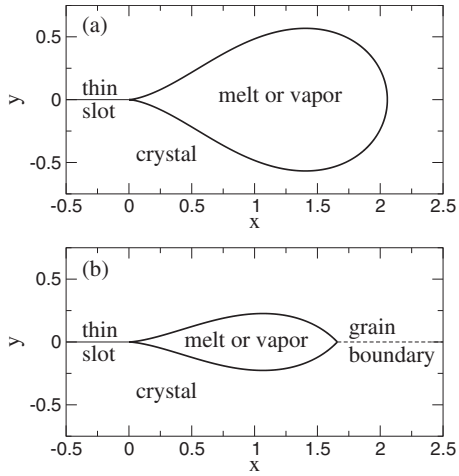

FIG. 3. Profiles of the traveling wave with $v=1$, for a = (a) 0.468 703 and (b) 0.3. The cavity moves to the left with speed $v=1$ without changing shape. The thin (in this limit, zero thickness) parallel-sided slot is shown as the line from $x=0$ along the negative real axis [which is the branch cut of Eq. (12)]. When $a \neq 0.468\,703$, the profile has a cusp on the right-hand side. This represents the (more realistic) solution when the thin slot terminates at a grain boundary between two crystals, rather than being a cavity in a single crystal.

$$y_0(x,t) \equiv v^{1/2}\hat{y}_0[v^{1/2}(x+vt);a], \tag{11}$$

where a is a real parameter which represents a constant of integration in Eqs. (6)–(8). Physically, a determines the curvature of the surface near to the tip of the teardrop-shaped cavity (the origin in Fig. 3).

After a considerable amount of back-substitution, one obtains (with the aid of MATHEMATICA [27]) a series solution for the analytic function $\hat{\psi}(z;a)$ and the real function $\hat{y}_0(x;a)$:

$$\hat{\psi}(z;a)=az^{-1/2}-\frac{a^3}{18}z^{1/2}-\frac{16}{15}z-\frac{5a^5}{1224}z^{3/2}-\frac{8a^2}{2835}z^2 -\left(\frac{7}{1950a}+\frac{1435a^7}{859\,248}\right)z^{5/2}+\frac{3328a^4}{2\,284\,443}z^3+O(z^{7/2}), \tag{12}$$

$$\pm\hat{y}_0(x;a)=\frac{4a}{3}x^{3/2}+\frac{38a^3}{27}x^{5/2}-\frac{8}{45}x^3+\frac{259a^5}{102}x^{7/2} -\frac{1336a^2}{1701}x^4+\left(\frac{10\,588\,243a^7}{1\,933\,308}-\frac{2}{8775a}\right)x^{9/2} -\frac{95\,801\,752a^4}{34\,266\,645}x^5+O(x^{11/2}). \tag{13}$$

The series solution for $\hat{y}_0(x)$ does not converge quickly enough to be useful. However, Eq. (12) for $\hat{\psi}(z)$ does converge quickly in the region of interest, and using this solution the profile $\hat{y}_0(x)$ can be drawn numerically, using Eq. (7). The results for two different values of the a parameter are shown in Fig. 3, and a graph of the enclosed area in Fig. 4.

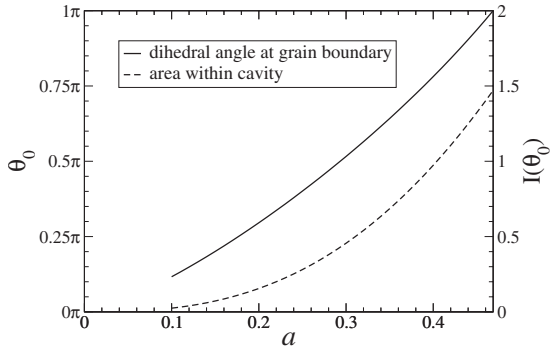

FIG. 4. Dihedral angle θ_0 at the grain boundary (if present) as a function of the parameter a (left-hand scale and solid curve). Enclosed area of the traveling wave cavity, defined by $I(\theta_0) \equiv \int 2\hat{y}_0[x;a(\theta_0)]dx$ (right-hand scale and dashed curve). Both plots are for a (nondimensional) wave velocity $v=1$.

Although the traveling wave solution just presented is an idealized case, an approximate analytical solution of this kind can also be used to construct the rate of neck growth in the original problem of two sintering spheres. This is done in the following manner. From Eqs. (10) and (11) we see that under magnification the velocity of the traveling wave is inversely proportional to its enclosed area, and is independent of the separation of the parallel surfaces in the initial slot-shaped cavity (provided this separation is very small). However, if the separation between these surfaces is not zero, then the teardrop-shaped cavity illustrated in Fig. 3 must grow in size as it moves, in order to maintain conservation of enclosed area (or volume in the three dimensional case), as discussed above. We note that, for the case of a neck growing between two touching spherical crystals, the teardrop cavity that will form (shown schematically in Fig. 5) is not a completely enclosed volume, but will be nearly so at early times.

Now suppose we have two spherical crystals with initial (nondimensionalized) diameters d_1 and d_2, which are brought into contact. Let the radius of the neck at (scaled) time t after contact be $r_n(t)$. The volume of material [to leading order in $r_n(t)/d_1$] that has been added to the crystals in order to make this solid neck is given by

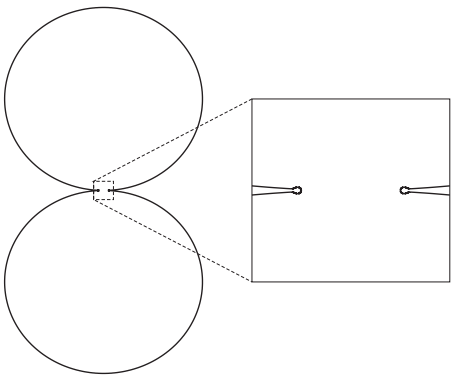

FIG. 5. Schematic illustration of where the traveling wave solution of Fig. 3 is expected to occur during the sintering of two spherical particles. Left-hand illustration shows the two crystals soon after contact. Right-hand panel shows a magnified portion of the neck region, with the teardrop traveling waves forming the edges of the neck.

$$\pi(d_1+d_2)r_n^4(t)/(2d_1d_2). \tag{14}$$

If we assume that the neck region forms a nearly completely enclosed volume, then the volume of crystal in this region must be conserved (using the argument from the divergence theorem above). The material used to make the solid neck must therefore come from the toroidal cavity formed by the traveling wave (illustrated schematically in Fig. 5).

We can estimate this volume using Eq. (11) and Pappus' second centroid theorem [22] (that the volume generated by rotating a plane figure around an axis is the product of its area and the distance moved by its centroid). The result (again to leading order) is

$$2\pi r_n(t)v^{-1}I(\theta_0), \tag{15}$$

where

$$I(\theta_0) \equiv \int 2\hat{y}_0(x;a)dx \tag{16}$$

is the enclosed area, which is a function of the equilibrium dihedral angle θ_0 at the grain boundary. The dihedral angle in turn is set by the grain boundary surface energy per unit area γ_{GB} through [14]

$$2\gamma\cos(\theta_0/2) = \gamma_{\mathrm{GB}}. \tag{17}$$

By equating the two volumes of Eqs. (14) and (15), we obtain the final result for the growth velocity of the neck at small times:

$$\frac{dr_n(t)}{dt} \approx \frac{2}{r_n^3}I(\theta_0)\frac{2d_1d_2}{d_1+d_2}, \tag{18}$$

so that $r_n(t) \propto t^{1/4}$.

III. SURFACE-DIFFUSION-LIMITED CASE

If recrystallization is limited by the rate of surface diffusion instead of bulk diffusion, then (still for the roughened, nearly isotropic γ case), the normal growth velocity of the crystal surface is given by [14]

$$v_n = v_n^S = \frac{\Omega_v^2 n_s D_s \gamma}{k_B T}\nabla_S^2\kappa, \tag{19}$$

where n_s is the number of molecules per unit area at the surface available to diffuse, D_s is a surface diffusivity, k_B is Boltzmann's constant, and ∇_S^2 is the surface Laplacian (also known as the Laplace-Beltrami operator [23]). Under the action of Eq. (19), the volume of the crystal is exactly conserved, which follows from the equivalent of the divergence theorem for ∇_S^2 [23].

In order to proceed, we nondimensionalize in a similar manner to that used in Sec. II. Let the coordinates of a point in space be denoted by $(\tilde{x},\tilde{y},\tilde{z})$ and time after contact by $\tilde{t}$. We define a capillary length $l_s \equiv \gamma\Omega_v/k_BT$ and dimensionless space and time variables $x=\tilde{x}/l_s$ and $t=\tilde{t}\Omega_v n_s D_s/l_s^3$. The equation for surface evolution then takes the nondimensionalized form

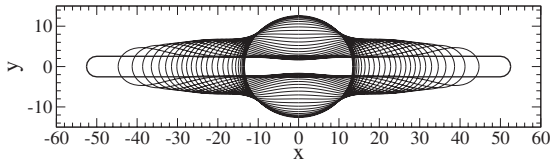

FIG. 6. Numerical solution for the surface-diffusion-limited evolution of a thin, parallel-sided, slot-shaped cavity in a crystal. The initial surface is shown in bold, and subsequent moments in time show the formation of dumbbell-shaped ends to the curve, before the final equilibrium shape is reached, which is a circle enclosing the same area as the original curve.

$$v_n = \nabla_S^2 \kappa. \tag{20}$$

If we again perform a simple, explicit numerical simulation for the evolution of a slot-shaped cavity in two dimensions, we obtain the results shown in Fig. 6.

This problem has in fact been studied before [24,25], in the context of the "inverse" case, where the authors study the evolution and breakup of a thin plate. However, since the evolution is determined by the surface only, this does not affect the equations. The formation of dumbbell-shaped ends in Fig. 6 is then the analog of the first stages of edge spheroidization of a plate [24,26].

Once more, this figure suggests that it is worth seeking a traveling wave solution to the evolution equation, which moves at constant velocity v without change of shape. To do this, we note that, if Θ is the angle that the curve representing the crystal surface makes with the y axis, s is the dimensionless distance along this curve and v is the dimensionless speed of propagation; then the relevant equation to solve is [from Eq. (20)]

$$v \cos \Theta = \frac{d^3\Theta(s)}{ds^3} \tag{21}$$

with the boundary condition $\Theta(0)=d^2\Theta(0)/ds^2=0$.

Figure 7 shows a numerical solution corresponding to $v=1$, while the form of Eq. (21) shows that, under magnification, the velocity v is proportional to the enclosed area to the power $-3/2$. Although a formal solution to Eq. (21), the curve is self-intersecting; indeed the asymptotic form for large negative x is

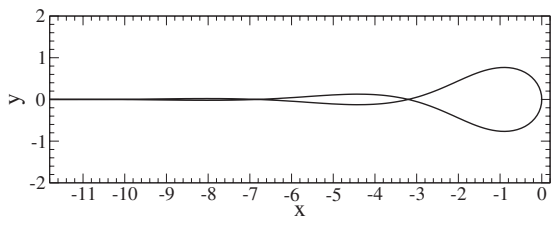

FIG. 7. Traveling wave solution for the equation of surface-diffusion-limited evolution [Eq. (20)]. The entire curve moves to the left at speed $v=1$. This is a purely mathematical solution to the problem, as the curve intersects itself and so cannot represent a real crystal boundary. The total (algebraic and nondimensionalized) area enclosed by the curve is 2.536

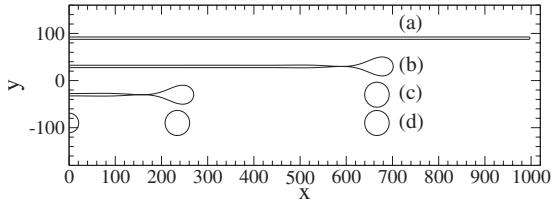

FIG. 8. Snapshots in time (displayed with vertical offset for clarity) for the evolution of an initial long slot-shaped cavity under surface-diffusion-limited evolution [Eq. (20)]. The initial cavity is shown in (a) and has a dimensionless width $w=16/\pi$. Configuration (b) is the first pinch-off event, at dimensionless time $t=2.17\times10^6$. Image (c) shows the second pinch-off event at $t=4.34\times10^6$ and (d) is the final, equilibrium configuration. Curves are drawn only for $x>0$, and are in fact symmetric under reflection about $x=0$.

$$y_0(x) \sim \pm e^{x/2} \cos(x\sqrt{3}/2). \tag{22}$$

This self-intersecting shape strongly suggests that under the evolution equation [Eq. (20)] a long slot-shaped cavity will repeatedly pinch off to form a string of equally spaced circular cavities in its wake. This behavior is indeed seen in the numerical simulation of a very long cavity in Fig. 8.

From the simulation results of Fig. 8 and the scaling properties of Eq. (21), we see that for a long slot-shaped cavity with a dimensionless separation w between the opposite, parallel crystal surfaces, the average (dimensionless) velocity of the end of the slot will be

$$\langle v \rangle \approx 0.0263 w^{-3}, \tag{23}$$

and the radius of each circle left behind in the wake is approximately $5.21w$.

For a pair of spherical crystals just after contact and evolving according to Eq. (20), it would be tempting to use Eq. (23), replacing w with the separation of the undisturbed spherical surfaces. This would give an average rate of growth of the radius r_n of the neck proportional to r_n^{-6}. However, this would be incorrect, as conservation of crystal volume is not taken into account properly. Instead, for the axisymmetric case of two spherical crystals each of (dimensionless) diameter d, we impose conservation of crystal volume in the following manner. First, assume that pinching off produces a series of concentric tori with major radii given by the set $\{r_i\}$ with $i \in \{1,2,\ldots\}$, and minor radii by the set $\{\rho_i\}$ given by

$$\rho_i \approx 5.21 w(r_i) \equiv 5.21(d - \sqrt{d^2 - 4r_i^2}) \tag{24}$$

[$w(r)$ being the separation of the surfaces of the original spheres at distance r radially from the initial contact point].

Conservation of enclosed volume then allows us to write down the distance from the axis of symmetry at which the ith torus lies [22]:

$$\int_{r_{i-1}}^{r_i} 2\pi r w(r) dr \approx 2\pi r_i \pi [5.21 w(r_i)]^2. \tag{25}$$

However, Eq. (25) has only one solution, namely,

$$r_1 \approx \frac{d}{8\pi(5.21)^2} \approx 0.001\ 47d. \tag{26}$$

We therefore expect the growing neck to leave behind one tiny toroidal cavity, before proceeding to grow without pinch-off events. We conjecture that this toroidal cavity will subsequently break up into a ring of spheres by a similar mechanism to the breakup of a cylinder [26] or edge spheroidization of a plate [24].

If, after this single pinch-off event, the profile still maintains a dumbbell-shaped end, similar to Fig. 8, and containing most of the volume of the vapor or melt in the neck region, then (again by conservation of enclosed volume and using the algebraic area in the curve of Fig. 7), the neck radius r_n should grow as

$$\frac{dr_n(t)}{dt} \approx \left(\frac{2 \times 2.536 r_n d}{r_n^4 - (0.001\ 47d)^4}\right)^{3/2}, \tag{27}$$

so that very approximately $r_n(t) \propto t^{1/3}$.

We note that grain boundaries are also easily incorporated into this formalism, by changing the value of $\Theta(0)$ in Eq. (21) to introduce the relevant dihedral angle at the origin in Fig. 7. Just as in Sec. II, the grain boundary runs parallel to the slot (and outside it), while in Ref. [24] the geometry is very different: grain boundaries run perpendicular to the plate (and inside it).

IV. CONCLUSIONS

For two sintering roughened crystals, the observation that the geometry near the contact point in the first moments after contact is two dimensional (and very similar to a slot-shaped cavity) is a considerable simplification for analyzing the problem at these early times. We are able to bring to bear complex analysis in the case of bulk-diffusion-limited crystal evolution, and simple numerical approaches for the surface-diffusion-limited case. The result is a different scaling for the power law for growth of the neck in the bulk-diffusion-limited case [namely, $r_n(t) \propto t^{1/4}$ from Eq. (18)], and the prediction of a pinch-off event [Eq. (26)] followed by approximately power law growth [Eq. (27)] for the surface-diffusion-limited case.

ACKNOWLEDGMENTS

The authors thank Ian Burns, Michael van Ginkel, Scott Singleton, Chris Clarke, Javier Aldazabal, and Aitor Luque for many useful discussions.

[1] G. Wulff, Z. Kristallogr. Mineral. **34**, 449 (1901).
[2] W. Kossel, Nachrichten von der Gesellschaft der Wissenschaften zu Göttingen aus dem jahre, p. 135 (1927).
[3] I. N. Stranski, Z. Phys. Chem. **136**, 259 (1928).
[4] E. D. Williams and N. C. Bartelt, Science **251**, 393 (1991).
[5] W. K. Burton, N. Cabrera, and F. C. Frank, Philos. Trans. R. Soc. London, Ser. A **243**, 299 (1951).
[6] A. Pavlovska and D. Nenow, Surf. Sci. **27**, 211 (1971).
[7] P. E. Wolf, S. Balibar, and F. Gallet, Phys. Rev. Lett. **51**, 1366 (1983).
[8] M. Elbaum, Phys. Rev. Lett. **67**, 2982 (1991).
[9] M. Maruyama, Y. Kishimoto, and T. Sawada, J. Cryst. Growth **172**, 521 (1997).
[10] T. Halpin-Healy and Y. C. Zhang, Phys. Rep. **254**, 215 (1995).
[11] A. M. Williamson, A. Lips, A. Clark, and D. Hall, Powder Technol. **121**, 74 (2001).
[12] A. Karma and W.-J. Rappel, Phys. Rev. E **57**, 4323 (1998).
[13] A. Barbieri and J. S. Langer, Phys. Rev. A **39**, 5314 (1989).
[14] W. W. Mullins, J. Appl. Phys. **28**, 333 (1957).
[15] H. Spohn, J. Phys. I **3**, 69 (1993).
[16] H. Pinkerton and R. S. J. Sparks, Nature (London) **276**, 383 (1978).
[17] M. Mellor, Cold Regions Sci. Technol. **3**, 305 (1980)
[18] T. H. Courtney, Metall. Trans. A **8**, 671 (1977).
[19] W. Ostwald, Z. Phys. Chem. **37**, 385 (1901).
[20] I. M. Lifshitz and V. V. Slyozov, J. Phys. Chem. Solids **19**, 35 (1961).
[21] C. Wagner, Z. Elektrochem. **65**, 581 (1961).
[22] F. Commandino, *Pappi Alexandrini Mathematicae Collectiones* (Franciscum de Franciscis Senensem, Venice, 1589).
[23] S. Iyanaga and Y. Kawada, *Encyclopedic Dictionary of Mathematics* (MIT Press, Cambridge, MA, 1980).
[24] J. K. Lee and T. H. Courtney, Metall. Trans. A **20**, 1385 (1989).
[25] J. C. Malzahn Kampe, T. H. Courtney, and Y. Leng, Acta Metall. **37**, 1735 (1989).
[26] F. A. Nichols and W. W. Mullins, J. Appl. Phys. **36**, 1826 (1965).
[27] http://www.wolfram.com